# Effect of Thermal Processes on Copper-Tin Alloys for Zinc Gettering

## M. Golyski

## P. Korinko

**Oct. 8, 2013**

**This Page Intentionally Left Blank**

## SRNL-STI-2013-00625

# Effect of Thermal Processes on Copper-Tin Alloys for Zinc Gettering

## Approvals

Signature on File

10/8/2013
Date

P. S. Korinko, Author
Materials Compatibility and Welding Technology

Signature on File

10/17/13
Date

M. Golyski, Author
Savannah River Tritium Enterprise

Signature on File

10/22/2013
Date

E.A. Clark, Technical Review
Materials Compatibility and Welding Technology

Signature on File

10/29/2013
Date

T. M. Adams, Manager
Materials Compatibility and Welding Technology

Signature on File

10/24/2013
Date

K.J. Stoner, TEF Engineer
Savannah River Tritium Enterprise

# Table of Contents

List of Tables ........ 4
List of Figures ........ 5
Summary ........ 6
Background ........ 6
Experimental ........ 7
  Sample Preparation ........ 7
  Oxidation Exposure ........ 9
  Reduction Exposures ........ 11
  Zinc exposure ........ 12
  Sample Characterization ........ 13
Results and Discussion ........ 13
  Sample Characterization ........ 13
  Oxidation Exposure ........ 14
  Reduction Exposure ........ 15
  Zinc Exposure ........ 18
Discussion ........ 22
Summary and Conclusion ........ 22
References ........ 22

# List of Tables

Table 1.Powder compositions with relative mass and percentage tin. ........ 9
Table 2.Sintering profile used. ........ 9
Table 3. Conditions used for oxidation exposures. ........ 11
Table 4. Composition of As-Fabricated samples. ........ 14
Table 5. Composition of the oxidized samples using SEM semi-quantitative techniques. ........ 17
Table 6. 450°C Oxidation Samples Reduced at 250°C ........ 17
Table 7. Oxides present in the as-fabricated and 450°C oxidized condition. ........ 17
Table 8. Mass change of samples after zinc exposure. ........ 21

# List of Figures

Figure 1. Analytic Scale used to weigh powders. 7
Figure 2. Pulverizer mill used to homogenize Cu-Sn powder blends. 7
Figure 3. 13 mm die used to compact powders. 8
Figure 4. Press used to compact the powders in the die. 8
Figure 6. Manual rolling mill used to thin the sintered samples. 8
Figure 5. Tube furnace used for sintering and oxidation exposures. 8
Figure 9. Successful oxidation scoping experiment, showing minimal discoloration of the samples after 350°C/12 hr exposure. 9
Figure 7. Sample appearance after initial scoping oxidation experiment. Note heavy discoloration on samples. 9
Figure 10. MS data for a typical oxidation exposure. 10
Figure 12. Flow control valves on the reduction apparatus. 11
Figure 13. Control valves on to direct gas to appropriate zone for the reduction apparatus. 11
Figure 11. Test cell and ceramic heater used for the reduction exposures. 11
Figure 14. Filter housing with samples inserted. 12
Figure 15. Filter housing heated with ceramic heater. 12
Figure 16. Thermal vacuum zinc deposition apparatus and instrumentation. 12
Figure 17. (a) as pressed, (b) as sintered and (c) as rolled condition of the pure copper pellets. 13
Figure 18. X-ray dot maps for the as-fabricated samples. 14
Figure 19. Appearance of samples after oxidation at indicated temperature. Each row consists of a Cu, Cu-1.25% Sn, Cu-2.5% Sn, and Cu-5% Sn sample. 14
Figure 20. Appearance of samples after oxidation and reduction showing the effect of temperature on the effectiveness of the treatment. Note dots indicate alloy and cuts indicate oxidation temperature. 15
Figure 21. Mass Spec data for a reduction exposure conducted at 350°C. 16
Figure 22. X-ray dot maps of the samples oxidized at 450°C and reduced at 250°C. 16
Figure 23. XRD pattern of Cu-5% Sn sample oxidized at 450°C. 18
Figure 24. Appearance of the samples reduced at 250°C after zinc exposure. 19
Figure 25. Appearance of the samples reduced at 350°C after zinc exposure. 19
Figure 26. Appearance of the samples reduced at 450°C after zinc exposure. 19
Figure 27. Appearance of the samples in the as-fabricated and as-oxidized condition after zinc exposure. 20
Figure 28. Mass change of samples in the as fabricated and as oxidized conditions. 20
Figure 29. Mass change of the reduced samples after zinc exposure. 21

## Summary

A contamination mitigation plan was initiated to address the discovery of radioactive zinc-65 in a glovebox. A near term solution was developed, installation of heated filters in the glovebox piping. This solution is effective at retaining the zinc in the currently contaminated area, but the gamma emitting contaminant is still present in a system designed for tritium beta. A project was initiated to develop a solution to contain the $^{65}$Zn in the furnace module. Copper and bronze (a Cu/Sn alloy) were found to be candidate materials to combine with zinc-65 vapor, using thermodynamic calculations. A series of binary Cu/Sn alloys were developed (after determining that commercial alloys were unacceptable), that were found to be effective traps of zinc vapor. The task described in this report was undertaken to determine if the bronze substrates would retain their zinc gettering capability after being exposed to simulated extraction conditions with oxidizing and reducing gases. Pure copper and three bronze alloys were prepared, exposed to varying oxidation conditions from 250 to 450°C, then exposed to varying reduction conditions in He-$H_2$ from 250-450°C, and finally exposed to zinc vapor at 350°C for four hours. The samples were characterized using scanning electron microscopy, X-ray diffraction, differential thermal analysis, mass change, and visual observation. It was observed that the as fabricated samples and the reduced samples all retained their zinc gettering capacity while samples in the “as-oxidized” condition exhibited losses in zinc gettering capacity. Over the range of conditions tested, i.e., composition, oxidation temperature, and reduction temperature, no particular sample composition appeared better. Samples reduced at 350°C exhibited the greatest zinc capacity, although there were some testing anomalies associated with these samples. This work clearly demonstrated that the zinc gettering was not adversely affected by exposure to simulated process conditions and a full scale lithium and zinc trap should be fabricated for testing in the Tritium Extraction Facility.

## Background

Radioactive zinc-65 ($^{65}$Zn) has been detected after TPBARs that were irradiated at TVA’s Watts Bar Nuclear Reactor were extracted in the Tritium Extraction Facility at the Savannah River Site. The radiation signature produced a gamma signature in TEF Glovebox 500 that was greater than background. Review of the potential sources of $^{65}$Zn from the TPBAR components indicates that the $^{65}$Zn is an activation product of natural zinc that is present as a minor contaminant in several of the TPBAR materials of construction. The results from the initial postmortem examination of the piping removed from the TEF, and a literature review of vapor phase deposition indicated that certain conditions may be beneficial to the growth of zinc whiskers (1, 2). Consequently 20 µm filters heated to 200°C were installed in the glovebox in key areas of the TEF process lines (3). The subsequent post-mortem examination of the filters, especially gamma scans, indicated that $^{65}$Zn had been trapped within these locations. The deposit morphology on several of the filters was difficult to characterize due to the small quantity of activated zinc and the presence of native Zn (non-radioactive) on the filters (4). The results of these examinations and early containment efforts lead TEF to sponsor an effort to optimize filter capturing and evaluate the possibility of capturing zinc within the lithium trap. An experimental program was initiated to develop and validate conditions to effectively trap Zn vapor released during extraction in the TEF (5). The first phase of the zinc mitigation efforts work was divided into three experimental tasks and a literature/thermodynamics study. The first experimental task was to determine the effect of pore size on pumping efficiency (6); the second was to determine the effectiveness of various pore sizes of filter elements to trap zinc vapor, which revealed that 20 µm filters would be effective to trap the zinc vapor (7); the third task was to determine the effect of filter temperature on zinc vapor deposition, which resulted in a recommendation that the filters be heated to between 120 and 200°C (8). The thermodynamics study indicated that copper and cobalt may be effective at trapping zinc in a chemical form while avoiding forming hydrides (9). The desired outcome is to capture the zinc in the furnace module and ideally in the lithium trap so that the $^{65}$Zn contamination is disposed of with the spent TPBARs. This approach reduces waste, reduces facility contamination, reduces maintenance, and maintains contamination in the areas that are designed to handle it. Since the thermodynamic study validated that copper and cobalt could potentially be used to chemically bind zinc vapor, and experimentally it was shown that copper will attract zinc vapor at higher temperatures than stainless steel. Because of the small amount of deposit, it was not possible to determine if the zinc reacted (10). Subsequently, a high vacuum system was constructed and tests were conducted using copper and commercially available bronzes which clearly demonstrated that it was feasible to capture and alloy copper based materials with zinc over a range of temperatures (11). Additional testing also demonstrated an unfortunate characteristic of these copper based materials by showing that the reaction for zinc alloying was reversible under high vacuum conditions at moderate temperatures (12). However, based on the cost and rate of decomposition copper based alloys are considered a suitable first choice for zinc capture.

Initially, commercial bronze alloys were tested and were shown to be effective (11). However, most commercial bronzes contain alloying and contamination elements that are incompatible with the extraction gas, such as phosphorous, or create mixed waste, such as lead. Consequently, an alloy development task was initiated to develop simple binary Cu-Sn alloys. Samples were prepared using powder metallurgy, solid state sintering, and subsequent rolling. Samples with 0 to 30 wt % tin were tested (13) and it was shown that there was no systematic effect of tin on the zinc gettering capability; however, tin was shown to be beneficial at all levels compared to pure copper. At tin concentrations as low as 5% there is an improvement in zinc capture and gettering, and there are potential adverse metallurgical effects of increasing Sn to levels greater than 10% with the development of multiphase alloys which can make it more difficult to mechanically work the alloys (14). Consequently, this work emphasized alloys with less than 10% Sn.

The purpose of these experiments was to determine the effect of passing an oxidizing and reducing gas over the samples and determining the residual gettering capacity of pure copper and copper having 1.25%, 2.5%, and 5% tin samples. Samples were prepared using powder metallurgical techniques, of blending, compaction, and sintering. The samples were cold rolled and ground, then oxidized by argon water gas, reduced in helium-hydrogen, and their zinc gettering capability tested in a high vacuum system at a single condition.

# Experimental

## Sample Preparation

Four copper-tin alloys were fabricated to test the reversibility of the samples to oxidize, reduce, and getter zinc. The compositions are listed in Table 1. The copper and tin powders were weighed on an analytic balance in 10 gram lots, Figure 1. A total of seven lots were prepared. Two lots of samples were pure Cu, two were Cu-1.25% Sn, one was Cu-2.5% Sn,

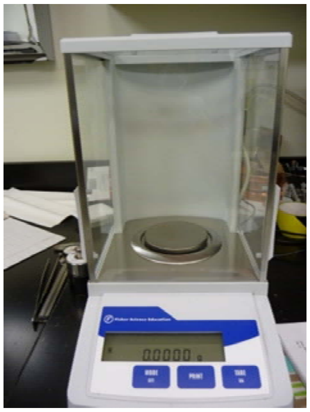

**Figure 1. Analytic Scale used to weigh powders.**

**Figure 2. Pulverizer mill used to homogenize Cu-Sn powder blends.**

and two were Cu-5.0% S. After the powders were combined, the powder blend was homogenized using the Pulverizer higher energy mill shown in Figure 2. Previous work (13) showed that it was necessary to mix the powders at 150 RPM for one hour then counter-clockwise at 150 RPM for an additional hour. Once the powders were thoroughly blended, nominally 0.5 grams samples were weighed, placed into a die shown in Figure 3 and uniaxially compressed to 10,000 and 11,600 pounds force using the hydraulic press shown in Figure 4 to prepare green compacts for sintering. The green (unsintered) pellets were placed on an alumina plate in 12 pellet lots and placed near the center of the tube furnace, Figure 6. The compacts were sintered using the thermal profile given in Table 2. Time and temperature data were recorded by computer during the sintering. After sintering the samples were weighed and measured and then the samples were cold rolled with a nominal reduction of 25% using the rolling mill shown in Figure 5. After rolling, any surface contamination and native oxide scale was removed from the samples by grinding them on 800 grit silicon carbide paper. The samples were ground until they showed uniform scratches, and low spots were locally dressed using a fine SiC grinding wheel with a rotary Dremel tool. After the surface preparation was complete, small holes were drilled in the center of each disk and each sample was marked with dots to indicate the alloy and edge marking to indicate the subsequent thermal treatments. Table 1 also shows the marking system used for the alloys.

**Figure 3. 13 mm die used to compact powders.**

**Figure 4. Press used to compact the powders in the die.**

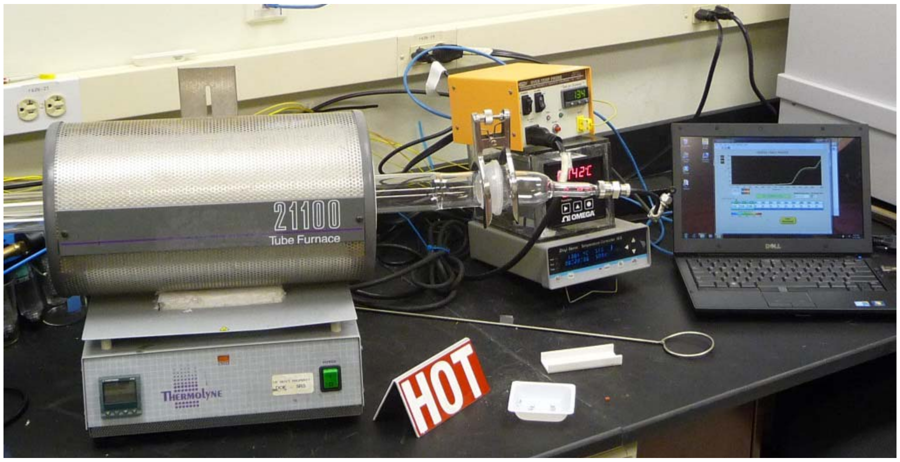

**Figure 6. Tube furnace used for sintering and oxidation exposures.**

**Figure 5. Manual rolling mill used to thin the sintered samples.**

Table 1.Powder compositions with relative mass and percentage tin.

| Nominal Composition (% Sn by mass, balance Cu) | Total Mass (g) | Mass Sn (g) | Percent Tin (%) | Marking |
|---|---|---|---|---|
| Cu 0 Sn | 10.0000 | 0 | 0.00 | None |
| Cu 1.25 Sn | 10.0000 | 0.1254 | 1.25 | One dot |
| Cu 1.25 Sn | 10.0100 | 0.1271 | 1.27 | One dot |
| Cu 2.5 Sn | 9.9806 | 0.2520 | 2.52 | Two dots |
| Cu 5 Sn | 10.2300 | 0.513 | 5.01 | Three dots |
| Cu 5 Sn | 10.0811 | 0.5423 | 5.40 | Three dots |

Table 2.Sintering profile used.

| Step | Temp | Time | Step | Temp | Time |
|---|---|---|---|---|---|
| 1 | 20 | 0:30 | 5 | 350 | 1:00 |
| 2 | 120 | 0:19 | 6 | 800 | 1:30 |
| 3 | 120 | 0:30 | 7 | 800 | 2:00 |
| 4 | 350 | 1:32 | 8 | 25 | 0:30 |

## Oxidation Exposure

A simple gas manifold that incorporated a water bubbler with a glass frit diffuser was assembled, shown in **Error! Reference source not found.**, and incorporated into the sintering furnace shown in Figure 6. The manifold included two rotameter flow controllers. A scoping study was conducted at 350°C to determine the length of time to conduct the Ar purge so that all the oxygen was displaced and only water vapor was present during the oxidation. The results from the scoping study are shown in Figure 8 and Figure 7. From Figure 8 it is apparent that the 45 minute purge and relatively low flow rate (60 sccm) was inadequate to displace the oxygen from the system so the room temperature purge duration was increased to 2 hours and the flow rate was increased. As seen in Figure 7, the 2 hour purge at 12 SCFH proved to be an effective duration and flow and was used for all further oxidation exposures. The scoping study also indicated that exposure to the oxidation temperature for 12 hours was sufficiently long to cause visible evidence of oxidation. The samples were weighed before and after exposure and were also photographed to document the condition. Based on the scoping study, the argon purge gas was set at 12.0 SCFH for two hours and the argon-water gas rotameter was set at 1.0 SCFH for the first two hours during an argon purge. The argon purge was used to displace all the air in the furnace tube and the water bath, with the water bath purge being exhausted to the room. At the end of two hours and for the oxidation exposure the flow meter of gas through the water bubbler was increased to 2.0 SCFH and the dry argon purge was terminated. To provide all the required samples for the test matrix, samples were oxidized in lots of 12 with four samples of each composition exposed in each oxidation run to support the

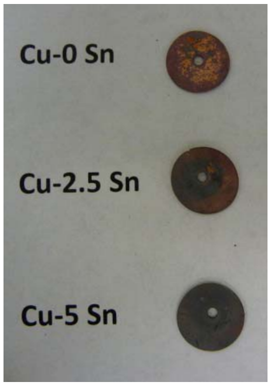

Figure 8. Sample appearance after initial scoping oxidation experiment. Note heavy discoloration on samples.

Figure 7. Successful oxidation scoping experiment, showing minimal discoloration of the samples after 350°C/12 hr exposure.

subsequent reduction exposure. The three oxidation exposures are listed in Table 3.

A mass spectrometer (MS) was used during the last few oxidation tests. The data in Fig. 10 are from a 250°C oxidation. The MS was used to characterize the water that was being cracked over the sample surfaces by monitoring hydrogen and oxygen (2 and 16 & 32 AMU) The MS was set up to capture the following gases: nitrogen, water vapor, oxygen, hydrogen and argon, Figure 9.

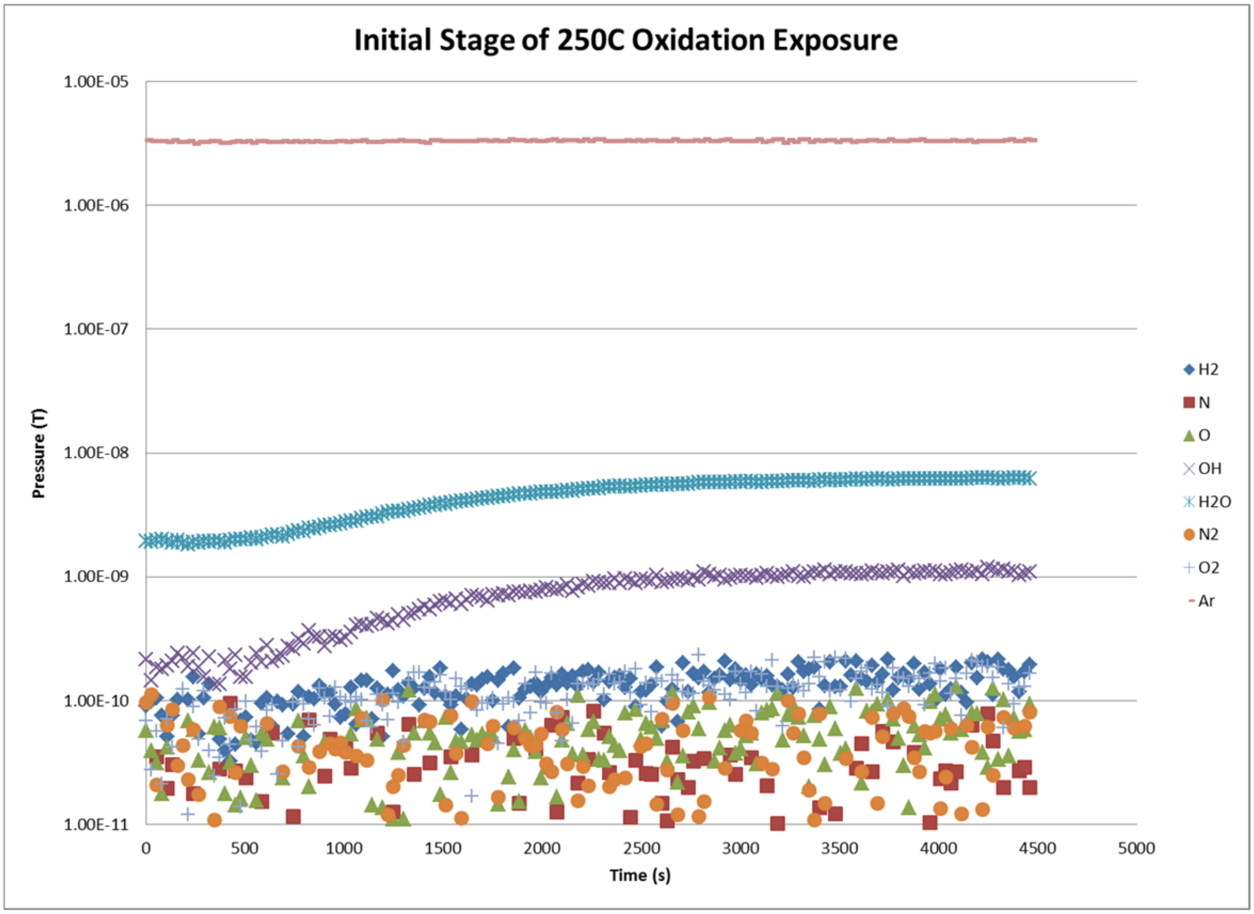

Figure 9. MS data for a typical oxidation exposure.

**Table 3. Conditions used for oxidation exposures.**

| Step | Time HH:MM | Initial Temperature (°C) | Final Temperature °C | Gas |
|---|---|---|---|---|
| 1 | 2:00 | 25 | 25 | Ar |
| 2 | 0:30 | 25 | 250, 350, or 450 | Ar+$H_2O$ |
| 3 | 12:00 | 250, 350, or 450 | 250, 350, or 450 | Ar+$H_2O$ |
| 4 | 0:45 | 250, 350, or 450 | 25 | Ar+$H_2O$ |

## Reduction Exposures

One sample from each compositional series, i.e., 0, 1.25, 2.5, and 5.0% Sn and from each oxidation exposure at 250°, 350°, and 450 °C for a total of 12 samples was subjected to a reduction exposure at each temperature, i.e., 250°, 350°, and 450 °C, in helium-5% hydrogen. Samples were loaded into a ¾" stainless steel tube with VCR-12 fittings, and the sample tube was connected to the manifold using copper gaskets and a ceramic heater was placed around the sample tube. The system was evacuated and backfilled three times with helium prior to heating. The apparatus used for the reduction exposure is shown in Figure 12, Figure 10, and Figure 11. The test cell was then brought up to temperature under helium and when the temperature stabilized the hydrogen flow was started. MKS mass flow controllers were used for the exposure. The target gas was He-5% $H_2$ which was achieved with a flow of 10% for the $H_2$ flow controller with a 500 sccm full scale (FS) reading and 47.5% for the He flow controller with a 2000 sccm full scale. Type K thermocouples were used as reference and control thermocouples. The tests were run for a minimum of 12 hours and were terminated manually. Samples were weighed and visually examined.

**Figure 12. Test cell and ceramic heater used for the reduction exposures.**

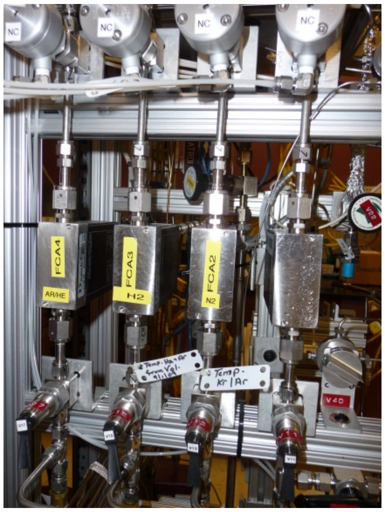

**Figure 10. Flow control valves on the reduction apparatus.**

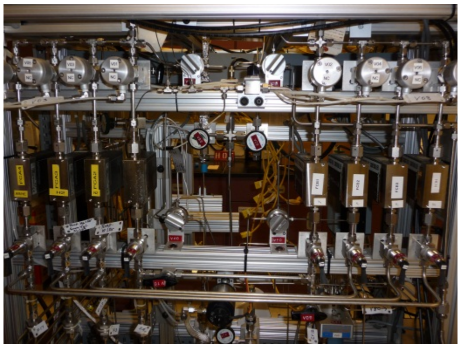

**Figure 11. Control valves on to direct gas to appropriate zone for the reduction apparatus.**

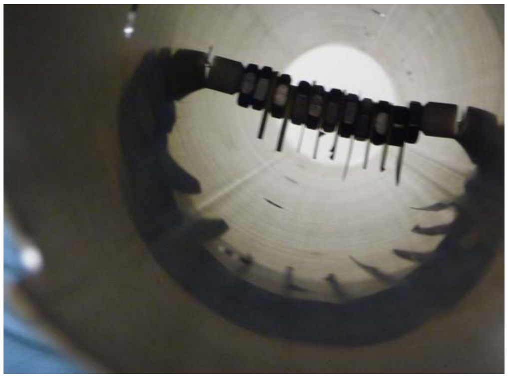

Figure 13. Filter housing with samples inserted.

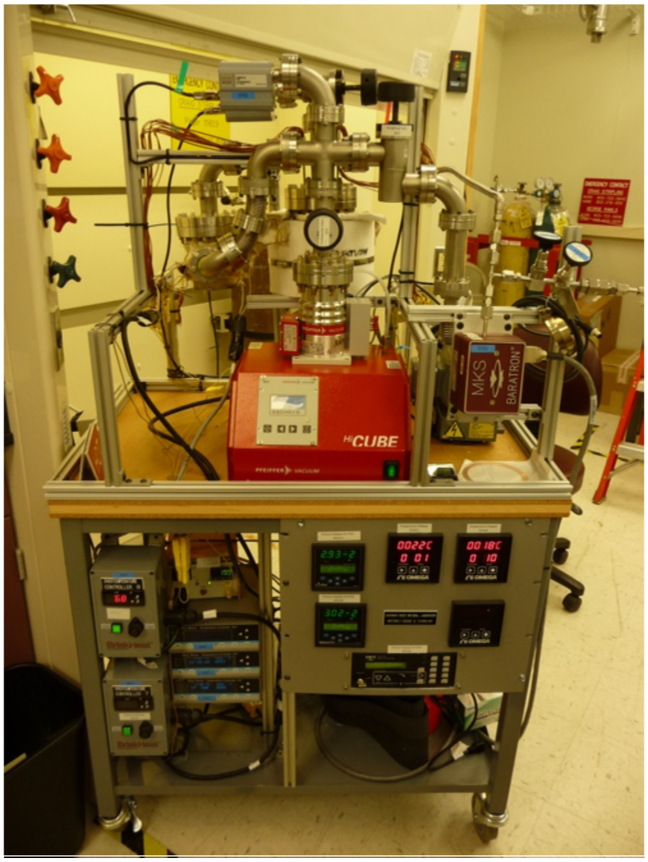

Figure 15. Thermal vacuum zinc deposition apparatus and instrumentation.

Figure 14. Filter housing heated with ceramic heater.

## Zinc exposure

The last experimental step was to test for the effectiveness of the copper-tin alloy to capture zinc after the samples were exposed to the simulated gases, i.e., water vapor and hydrogen. The test apparatus used is shown in Figure 15 An all metal seal (using Conflat Flanges) high vacuum deposition and capture system was designed and fabricated primarily from off-the-shelf components. Photographs of the filter holder with samples and heater section of the apparatus are shown in Figure 13 and 15 respectively. This system has a four inch half nipple that is used as a “zinc pot”. The zinc pot is connected to a full nipple that contains the zinc filter support. A wide range pressure gauge (KJ Lesker Pirani – hot cathode (WRG)) was placed above the zinc pot and a 10 Torr Baratron pressure transducer was connected to this chamber as well. The system was subsequently pumped through a 200°C heated trap that contained steel wool. The trap was heated using heater tape with three thermocouples attached for control, over-temperature and reference. A scroll pump was used to rough pump the system and turbo molecular pump used to achieve high vacuum ($P<1x10^{-5}$ Torr). A second wide range gauge was mounted over the turbo molecular pump. A mantle heater was used to heat the zinc pot to 350°C. The Zn pot had three type K thermocouples attached, one for control, one over-temperature and one reference. The filter is heated with a Watlow split cylinder ceramic fiber heater. It was insulated with ceramic wool. Four type K thermocouples were installed on the filter hot zone, one control, one over-temperature, and two reference thermocouples, one positioned at the top of the filter and the second positioned at the bottom. The internal temperature of the zinc pot and filter was monitored using an Omega thermocouple reader that reads twelve thermocouples. Two ten thermocouple element assemblies with thermocouples spaced 1.25 inches apart were read on channels 1-10. The filter was nominally positioned between the seventh and eighth elements. Channels 11 and 12 were used to monitor other temperatures on the assembly. Tests were conducted using written R&D Directions (4). Zinc was weighed and placed in the zinc pot. The system was evacuated for a minimum of 12 hours after reassembly to ensure that acceptable vacuum levels were achieved. The base vacuum, as measured by the WRG over the turbo molecular pump, was typically in the mid $10^{-7}$ Torr range prior to starting a test. The heaters were programmed so that they automatically heated at the desired rate and held for the target time. The trap was heated at 20°C/min to 200°C and held for 9 hours - 25 minutes, the filter was heated to the desired set point in 45 minutes and held for 9 hours, and the zinc pot was heated at 8 to 10°C/min to 350°C after a four hour delay for the filter area to reach its steady state temperature. The temperature and pressure data were recorded at approximately 15 second intervals using a custom Labview data acquisition program. Tests were run to a filter temperature of 350°C. After the system cooled, the apparatus was brought up to atmospheric pressure by venting with helium. The samples were removed and weighed on an Ohaus Discovery analytical scale and photographed using a Panasonic Lumix LZ5 digital camera.

### Sample Characterization

Samples were characterized using an Hitachi TM 3000 tabletop scanning electron microscope with images taken from 500-3000X magnification, with an accelerating voltage of 15 keV, the nominal working distance was 8mm, and the samples were characterized using X-ray energy dispersive spectroscopy at nominally 1000X and 3000X magnifications.

A Rigaku table top XRD was used to characterize the as fabricated and oxidized samples. Copper $K_\alpha$ X-rays were used. The samples were placed on a glass screen such that they were in the correct plane for diffraction. The samples were characterized manually based on 2θ position and the knowledge that only copper, tin, and oxygen were present.

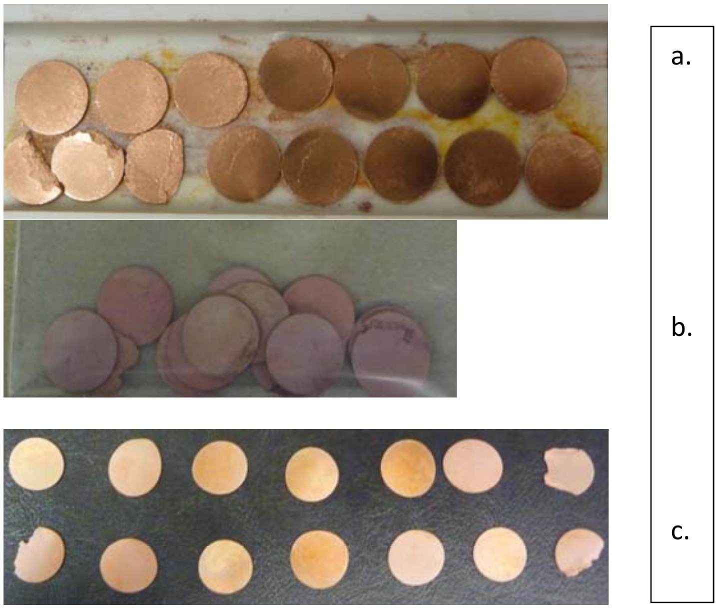

Figure 16. (a) as pressed, (b) as sintered and (c) as rolled condition of the pure copper pellets.

## Results and Discussion

### Sample Characterization

The appearance of selected as-pressed (i.e., green), as sintered and rolled samples are shown in Figure

16a-c. These samples exhibit a reddish tint on fabrication and rolling which is removed during the grinding step. There were localized areas that had to be dressed using a Dremel tool and these exhibited slightly rougher surfaces. The pre-test samples were characterized using the SEM and XRD to determine the oxygen content and phases present prior to oxidation, reduction, and zincification exposures. The X-ray dot maps for the samples of each composition are shown in Figure 17a-d. These results indicate that there is some oxygen present on the surface in addition to the regions that may be tin rich and the semi-quantitative results listing the compositions are shown in Table 4.

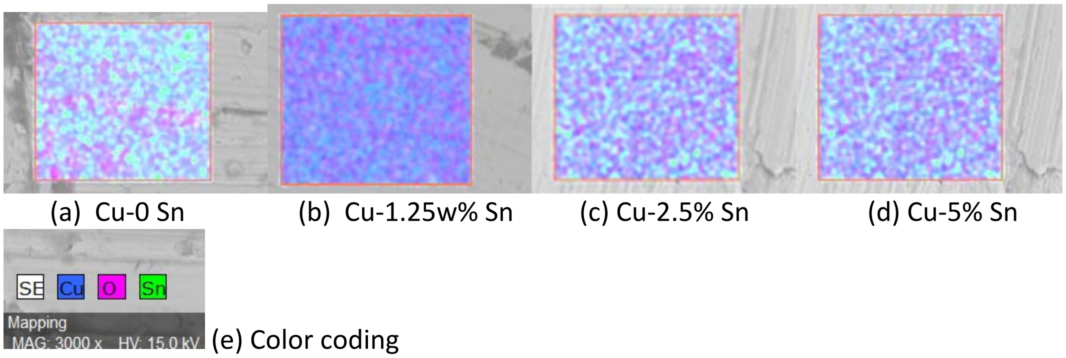

(a) Cu-0 Sn (b) Cu-1.25w% Sn (c) Cu-2.5% Sn (d) Cu-5% Sn

(e) Color coding

Figure 17. X-ray dot maps for the as-fabricated samples.

Table 4. Composition of As-Fabricated samples.

| As Fabrciated | Cu (wt %) | Sn wt (%) | O (Wt %) |
|---|---|---|---|
| Cu | 95.89 | 0.43 | 3.68 |
| Cu-1.25% Sn | 96.84 | 1.19 | 1.96 |
| Cu-2.5% Sn | 94.07 | 4.03 | 1.90 |
| Cu-5% Sn | 91.93 | 4.76 | 3.31 |

## Oxidation Exposure

The oxidation exposures showed that the conditions used resulted in increasing levels of oxidation with increasing temperature, as expected. The tarnish on the samples is greater for the 450°C than for the 250°C, Figure 18. In addition, the level of discoloration increases with increasing alloy content; with the Cu-5% Sn sample oxidized at 450°C being the darkest.

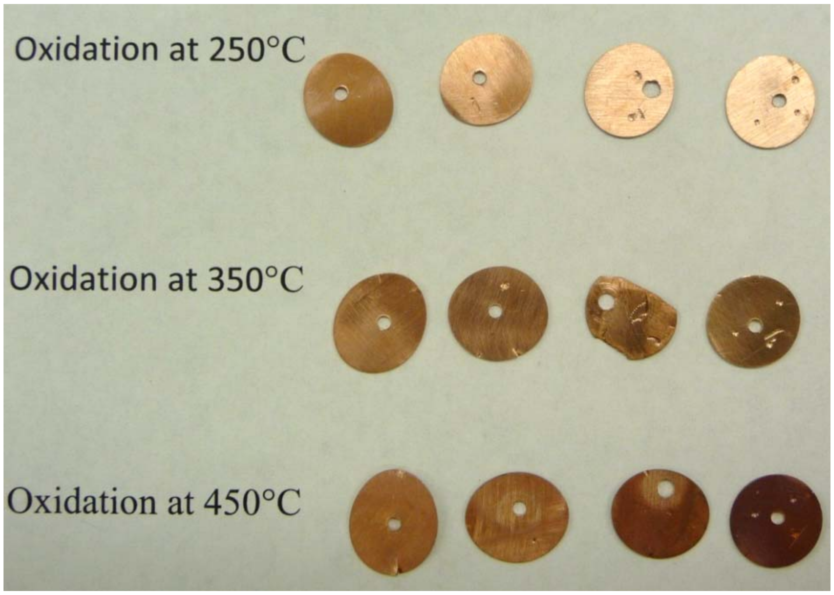

Figure 18. Appearance of samples after oxidation at indicated temperature. Each row consists of a Cu, Cu-1.25% Sn, Cu-2.5% Sn, and Cu-5% Sn sample.

## Reduction Exposure

All of the reduction exposures resulted in decreased levels of discoloration on the surface than what they appeared initially. The surface condition for the 250°C and 450°C reduction exposures are shown in Figure 19. These images indicate that there is more residual discoloration for the samples reduced at 250 °C than for the samples reduced at 450°C. This result is consistent with the expected increased thermodynamic and kinetic reactions that will occur with increasing temperatures. Included in the sample images are the effects of tin content and oxidation temperature, since one sample from each composition and oxidation condition were reduced at each temperature.

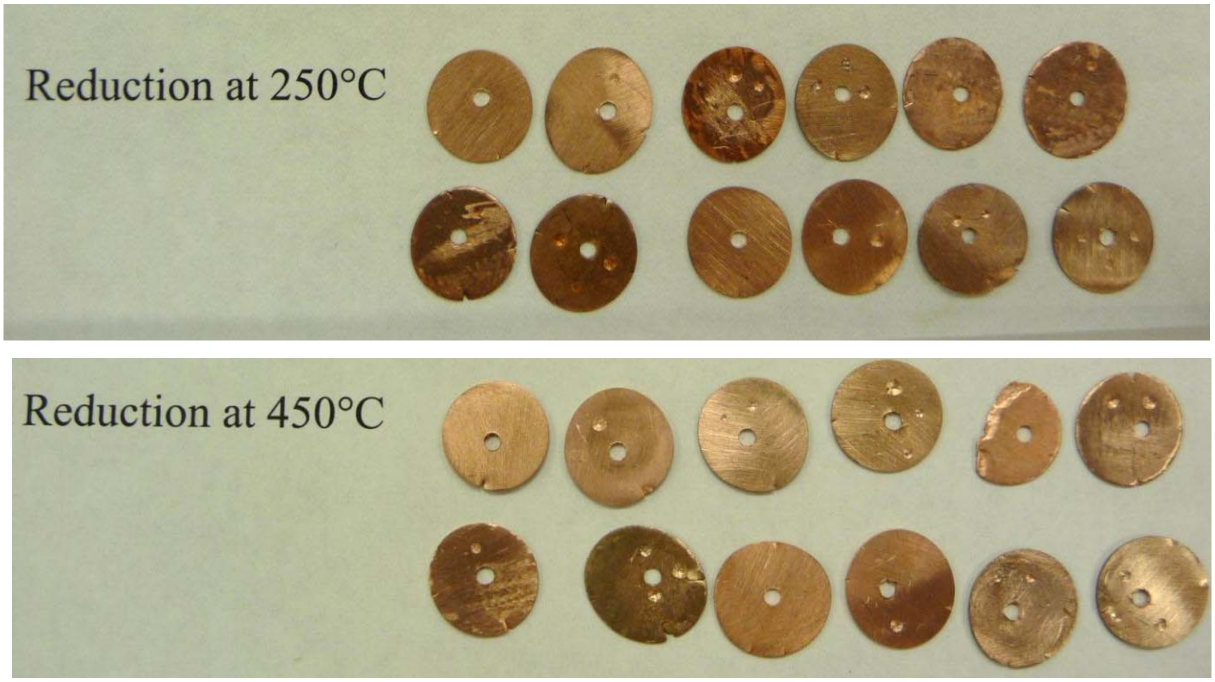

**Figure 19. Appearance of samples after oxidation and reduction showing the effect of temperature on the effectiveness of the treatment. Note dots indicate alloy and cuts indicate oxidation temperature.**

One experiment was conducted with a mass spectrometer to characterize the gas species as the reactions occurred. In this experiment, the presence of water initially increased when hydrogen was introduced and then subsequently decreased with further exposure to the reducing gas and ultimately achieved a value similar to the initial value for water, as shown by Figure 21.

Selected oxidized samples were examined on the scanning electron microscope (SEM) to characterize the surface morphology and determine oxygen content to compare with the as fabricated condition.

Table 5 shows the composition of selected samples after oxidation. Generally, the oxygen content increased as the temperature of the oxidation exposure increased. It also increased as the tin content of the sample increased, although there is not a one-to-one correlation for these data. In large part, this is likely due to the random nature of the sample selection and random selections for the region of interest for the analysis.

To further quantify the oxidation and reduction results, selected samples that were oxidized at 450°C and reduced at either 250°C or 450°C were also characterized. Figure 21 shows the X-ray false-color composition maps for the samples. There is a fairly uniform coloration with no apparent rich areas for either tin or oxygen. Table 6 shows the composition of the samples shown in Figure 22, i.e., samples oxidized at 450°C and reduced at 250°C. In general, the oxygen content decreased after the reduction step, except for the Cu-5% Sn sample which exhibited higher oxygen content after reduction, as noted by the highlighted cell in the table. Since the samples were not examined in exactly the same area, this difference is likely due to region to region differences that exist on the samples. Due to temporal restraints, only a single region on each sample was analyzed.

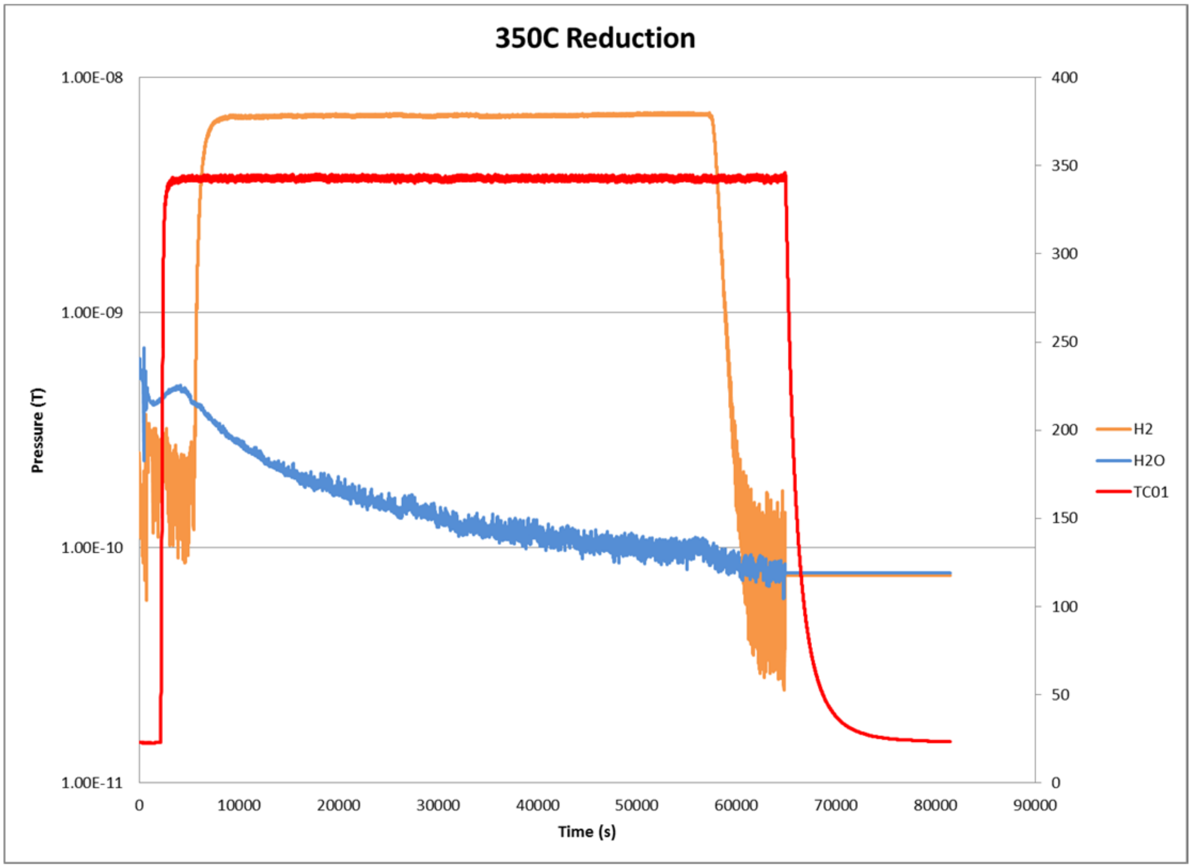

Figure 20. Mass Spec data for a reduction exposure conducted at 350°C.

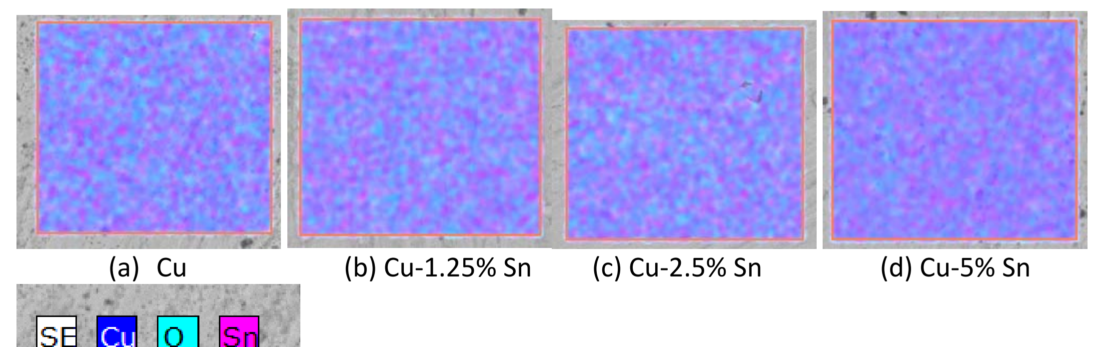
(a) Cu
(b) Cu-1.25% Sn
(c) Cu-2.5% Sn
(d) Cu-5% Sn

Table 5. Composition of the oxidized samples using SEM semi-quantitative techniques.

| Composition | Oxidation Temp °C | Copper (wt. %) | Tin (wt. %) | Oxygen (wt. %) |
|---|---|---|---|---|
| 0 Sn | 250 | 98.17 | 0.19 | 1.65 |
| 1.25 Sn | 250 | 97.71 | 1.12 | 1.17 |
| 2.5 Sn | 250 | 93.70 | 3.88 | 2.43 |
| 5.0 Sn | 250 | 94.05 | 4.21 | 1.74 |
| 0 Sn | 350 | NA | NA | NA |
| 1.25 Sn | 350 | 97.76 | 0.83 | 1.41 |
| 2.5 Sn | 350 | 92.43 | 4.25 | 3.32 |
| 5.0 Sn | 350 | 93.78 | 4.03 | 2.19 |
| 0 Sn | 450 | 97.33 | 0.98 | 1.71 |
| 1.25 Sn | 450 | 95.96 | 1.71 | 2.34 |
| 2.5 Sn | 450 | 93.98 | 3.58 | 2.44 |
| 5.0 Sn | 450 | 93.75 | 4.71 | 1.53 |

Table 6. 450°C Oxidation Samples Reduced at 250°C

| As Fabricated | Cu (wt %) | Sn wt (%) | O (Wt %) |
|---|---|---|---|
| Cu 450C Ox | 98.69 | 0.0 | 1.31 |
| Cu-1.25% Sn 450C Ox | 95.96 | 2.04 | 1.99 |
| Cu-2.5% Sn 450C Ox | 96.63 | 2.15 | 1.22 |
| Cu-5% Sn 450C Ox | 91.68 | 5.59 | 2.73 |

The samples were also examined using x-ray diffraction (XRD). Based on the analysis of the diffraction data, the specific oxides present on the samples could be ascertained. The XRD pattern for one of the Cu-5% Sn samples oxidized at 450°C is shown in Figure 22. This sample exhibits small amounts of SnO and CuO. The other samples oxidized at 450°C were also examined using the XRD with the results indicated Table 7.

Table 7. Oxides present in the as-fabricated and 450°C oxidized condition.

| **Sample ID** | **Oxides** |
|---|---|
| Cu 0 Sn As Fab | $SnO_2$ |
| Cu 0 Sn 450 Oxidation | $Cu_2$ O and CuO |
| Cu 1.25 Sn As Fab | $Cu_2O$ |
| Cu 1.25 Sn 450 Oxidation | $SnO_2$ |
| Cu 2.5 Sn As Fab | $SnO_2$ and $Cu_2O$ |
| Cu 2.5 Sn 450 Oxidation | $SnO_2$ |
| Cu 5.0 Sn As Fab | $SnO_2$ |
| Cu 5.0 Sn 450 Oxidation | $SnO_2$ and CuO |

The oxides that were detected are consistent with the oxidation conditions and sample chemistry with the exception of the pure copper sample. This sample exhibits the presence of tin oxide and can likely be explained by cross contamination that may have occurred either during the pressing and sintering steps since the same die and plungers were used for compaction adnd the same platen was used for sintering, or during the analysis phase since samples were mounted on the same supports for SEM and XRD.

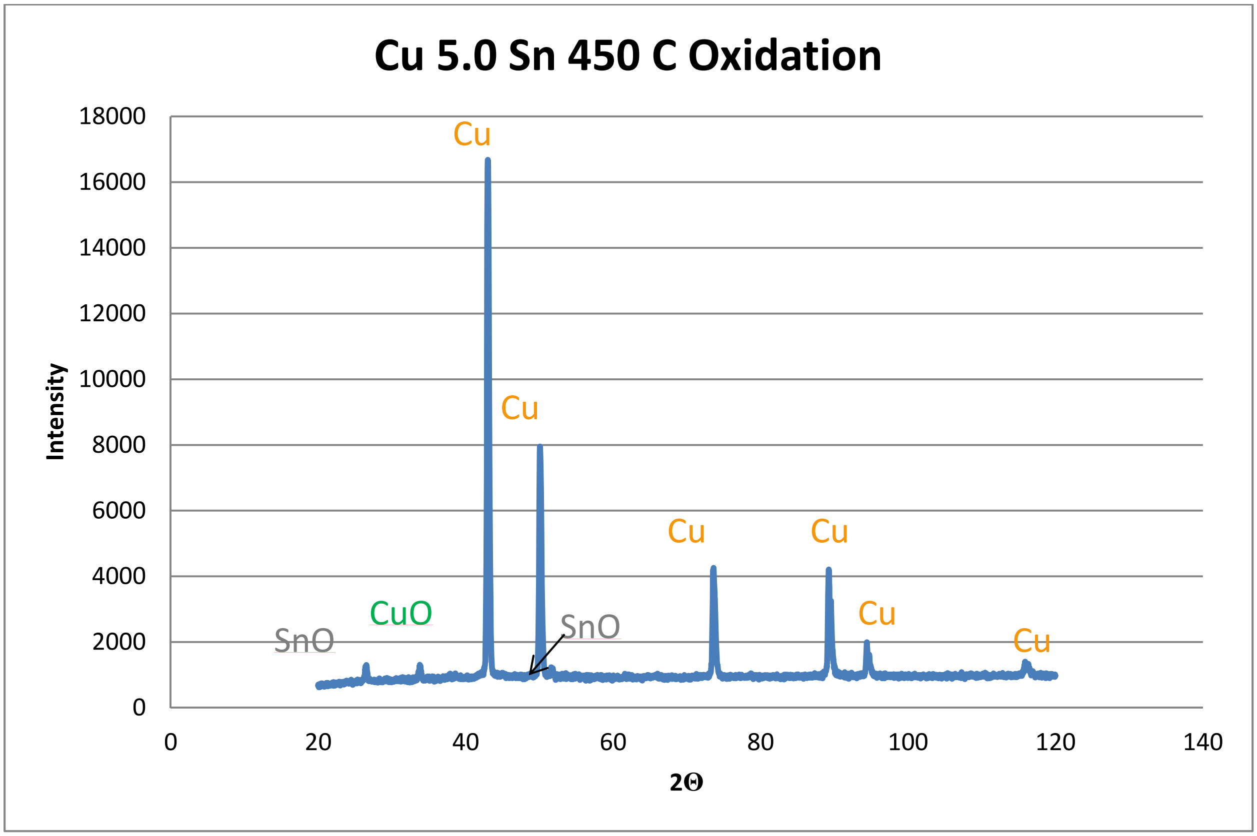

Figure 22. XRD pattern of Cu-5% Sn sample oxidized at 450°C.

## Zinc Exposure

Each lot of samples that were reduced, including an as fabricated and as oxidized lot, was subjected to zinc vapor exposure at 350°C with a zinc source temperature also at 350°C, conditions that were successfully used for previous experimentation (2). Due to an over-temperature event or controller malfunction, the 350°C reduction samples were exposed to two zinc deposition conditions. The first was an aborted zinc exposure that did not produce much weight gain followed by a standard exposure. This may partially explain the increased weights compared to the other conditions. Due to time constraints, duplicate tests were not conducted. The surface condition of the samples can be seen in Figure 23-Figure 26. There is visual evidence of zinc capture on most of the samples, with the exception of several of the 250°C reduction and as-oxidized samples. The weight gain for each of the samples is indicated in Table 8. These show that some gain was achieved for all but the pure copper as fabricated sample. This result is consistent for pure copper samples tested previously (2). The mass changes are shown graphically in Figure 27 andFigure 28. There is not a systematic variation of the sample weight gains either with reduction condition or surface treatment. This result is encouraging since it appears that slight oxidation products on the surface do not adversely affect the bronze material affinity to capture zinc. The higher than expected mass gain from the 350°C reduction after the dual exposure suggests that an alloy modification that includes zinc may prove beneficial.

Figure 23. Appearance of the samples reduced at 250°C after zinc exposure.

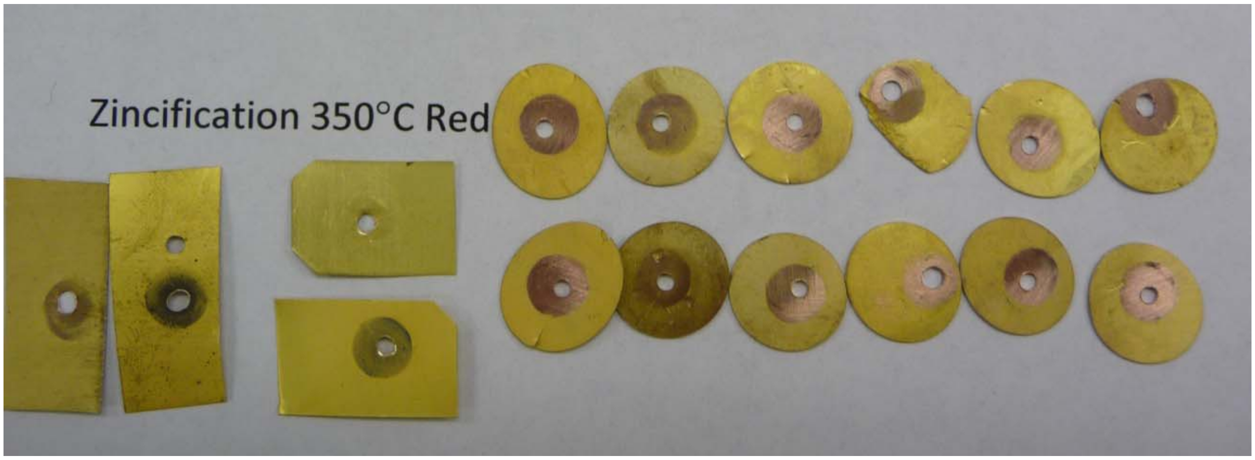

Figure 24. Appearance of the samples reduced at 350°C after zinc exposure.

Figure 25. Appearance of the samples reduced at 450°C after zinc exposure.

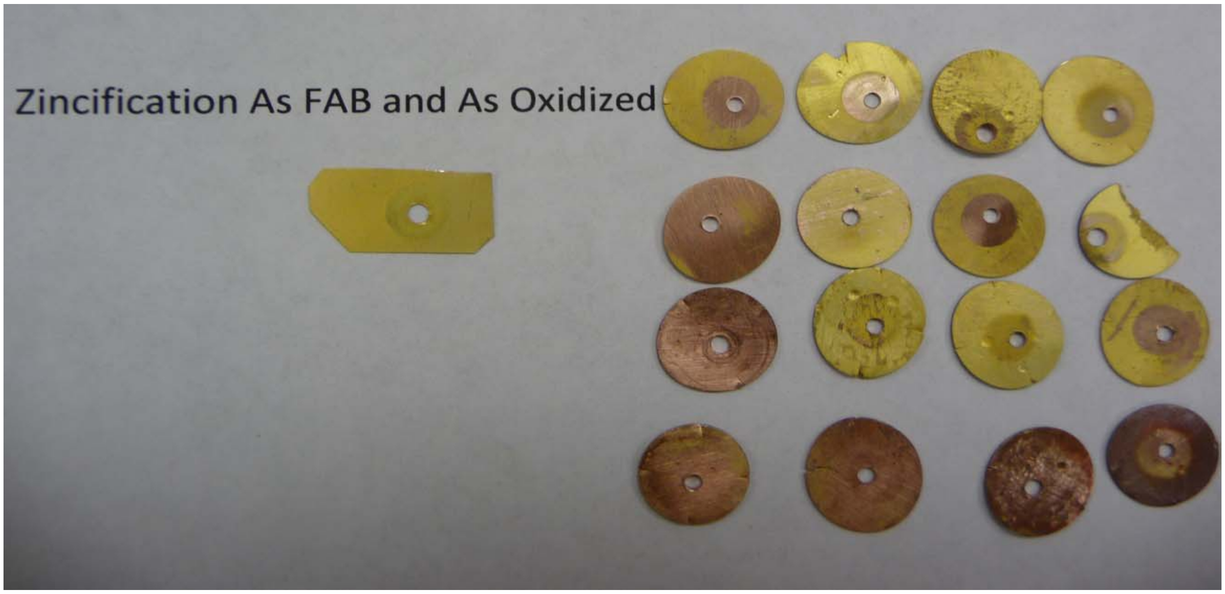

Figure 26. Appearance of the samples in the as-fabricated and as-oxidized condition after zinc exposure.

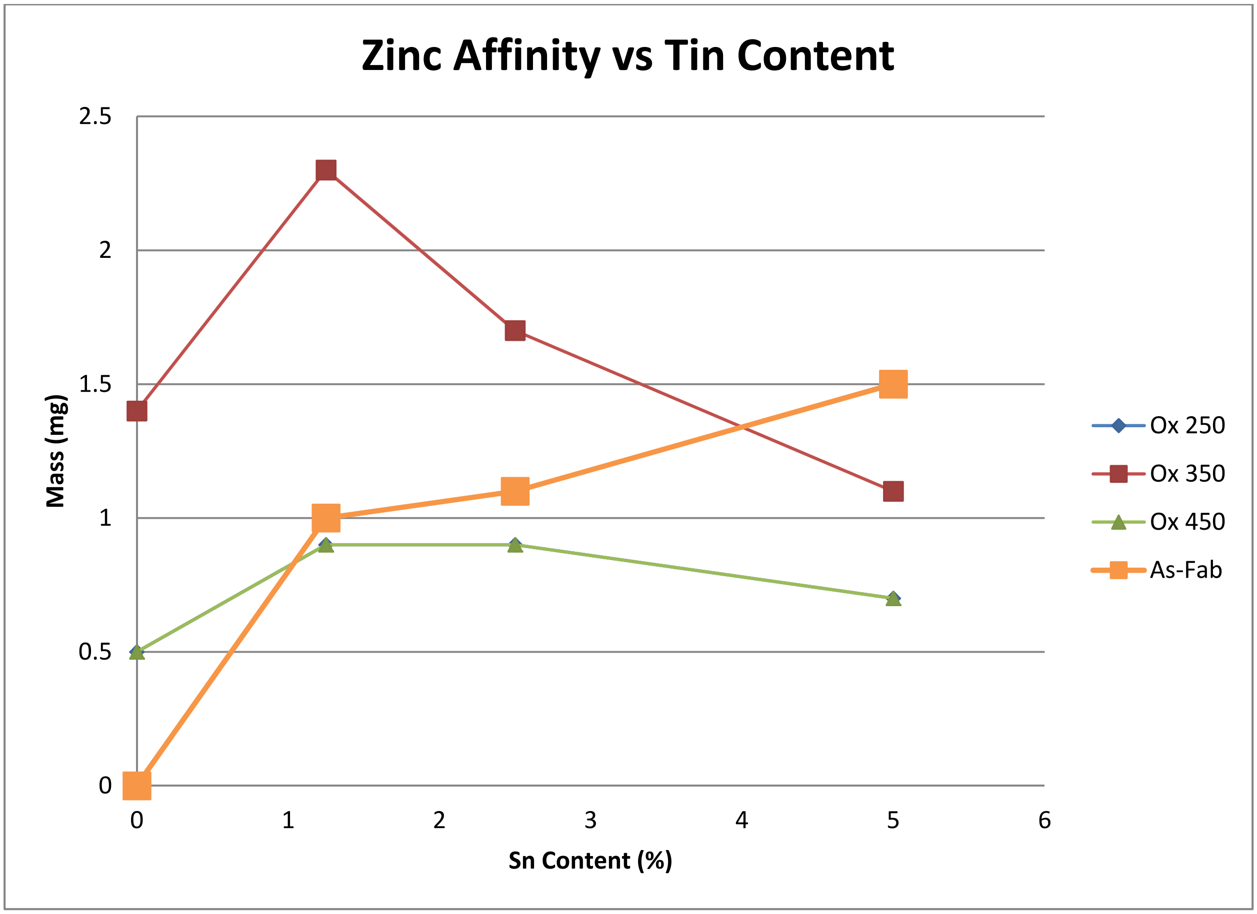

Figure 27. Mass change of samples in the as fabricated and as oxidized conditions.

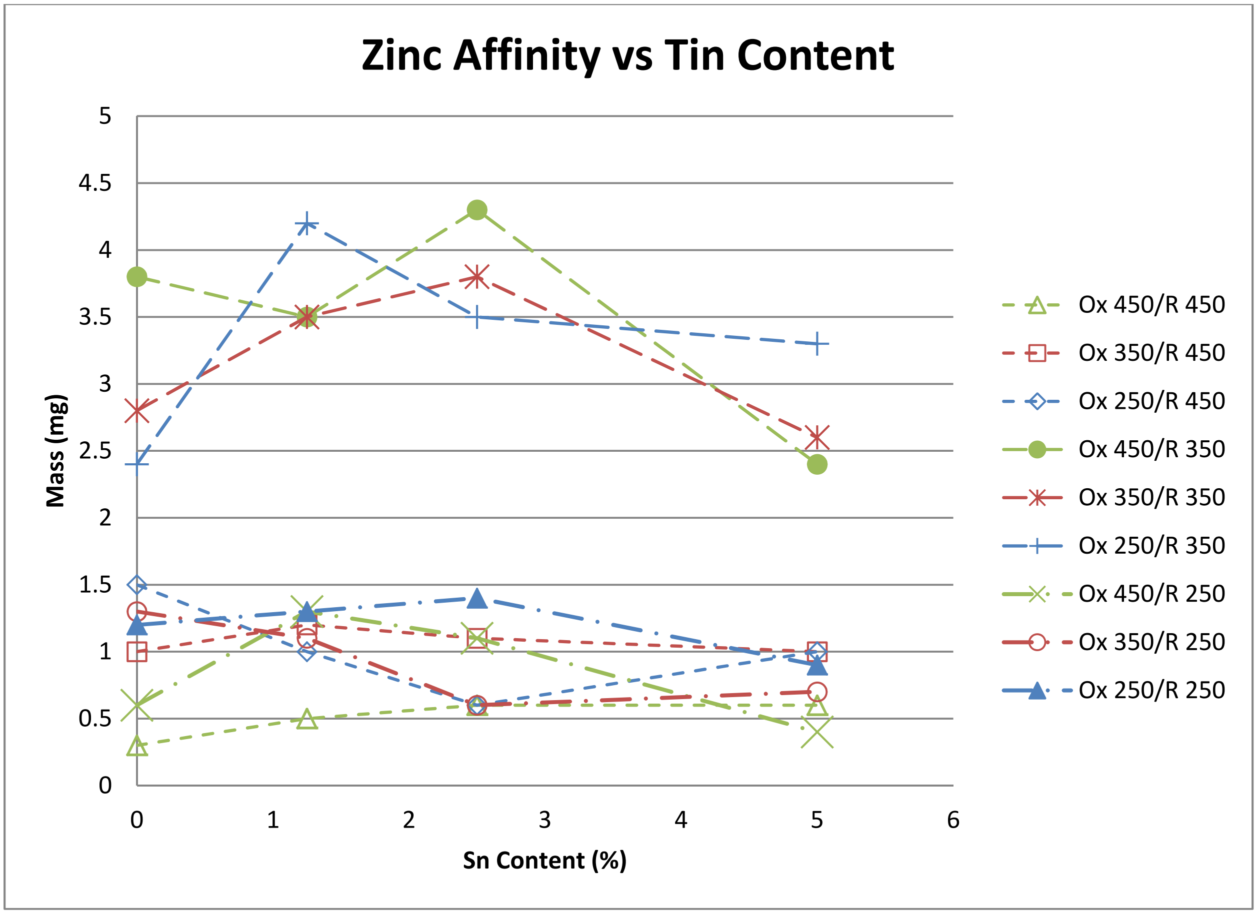

**Figure 28. Mass change of the reduced samples after zinc exposure.**

**Table 8. Mass change of samples after zinc exposure.**

| | | Temp ($^{o}$C) | | | 250C Reduction | | |
|---|---|---|---|---|---|---|---|
| % Sn | As-Fab | Ox 250 | Ox 350 | Ox 450 | Ox 250 | Ox 350 | Ox 450 |
| 0 | 0 | 0.5 | 1.4 | 0.5 | 0.6 | 1.3 | 1.2 |
| 1.25 | 1 | 0.9 | 2.3 | 0.9 | 1.3 | 1.1 | 1.3 |
| 2.5 | 1.1 | 0.9 | 1.7 | 0.9 | 1.1 | 0.6 | 1.4 |
| 5 | 1.5 | 0.7 | 1.1 | 0.7 | 0.4 | 0.7 | 0.9 |
| | 350C Reduction | | | | 450C Reduction | | |
| % Sn | Ox 250 | Ox 350 | Ox 450 | % Sn | Ox 250 | Ox 350 | Ox 450 |
| 0 | 3.8 | 2.8 | 2.4 | 0 | 0.3 | 1 | 1.5 |
| 1.25 | 3.5 | 3.5 | 4.2 | 1.25 | 0.5 | 1.2 | 1 |
| 2.5 | 4.3 | 3.8 | 3.5 | 2.5 | 0.6 | 1.1 | 0.6 |
| 5 | 2.4 | 2.6 | 3.3 | 5 | 0.6 | 1 | 1 |

## Discussion

This series of experiments combined with the previous experimentation for zinc capture indicate that bronze alloys provide a zinc active substrate that is active over a temperature range of 250°C to 450°C. These data coupled with the fabrication and preparation methods developed in this project indicate that a prototype zinc and lithium trap should be tested in the TEF. There are still challenges related to the long term stability of the captured zinc that need to be addressed, however, the simple bronze based alloy should reduce the amount of zinc that is released to the glovebox and could readily be scaled up for a full scale test.

## Summary and Conclusion

A series of experiments produced bronze coupons using powder metallurgy/sintering methods. Exposing these coupons to oxidation, reduction, and zincification respectively revealed that the samples can be oxidized and reduced successfully in a hydrogen environment. The samples still remain active for zinc capture. Samples in the as-oxidized condition also remained active, based on weight change data, but did not visually appear to turn gold, which is an excellent visual indicator for zinc capture. The bronze alloys appear to be a viable candidate for zinc capture.

Additional testing to determine if minor zinc additions to the bronze alloy will enhance the zinc capturing ability, as was indicated by the 350°C reduction experiment, would be worthwhile. In addition, modifications to the substrate materials that would limit the reversibility of the zinc capture and release should also be pursued, but these experiments can occur concurrently with design of a modified lithium trap.

## References

1. SRNL-STI-2011-00472, Summary Report for Zinc 65 Contamination Control, P. Korinko, 6/2011
2. SRNL-STI-2012-00616, Effectiveness of Copper and Bronze for Zinc Capture, P. Korinko, 10/2012
3. *Analysis of Zinc 65 Contamination After Vacuum Thermal Process*, Paul S. Korinko & Michael H. Tosten, J Fail. Anal. and Preven. Volume 13, Number 4, 13:389-395
4. SRNL-L7100-2008-00001, Analysis of TEF Pipe with Zn-65 Contamination, P. Korinko, M. Tosten, Z. Nelson, Sept. 2008.
5. SRNL-L4400-2010-00003, Zinc Mitigation Interim Report -- Effect of Pore Size, P. Korinko, 12/2010.
6. SRNL-L4410-2011-00008, Zinc Mitigation Interim Report -- Effect of Filter Temperature on Trapping, 3/2011.
7. SRNL-L4410-2010-00001, Zinc Mitigation Interim Report – Thermodynamic Study, P.S. Korinko, 12/2010.
8. SRNL-L4410-2011-00020, Zinc Mitigation Interim Report – Preliminary Study of Chemically Binding Zinc, P.S. Korinko, 6/2011
9. SRNL-L7100-2008-00001, Analysis of TEF Pipe with $^{65}$Zn Contamination P. Korinko, M. Tosten, Z. Nelson, 9/2008.
10. TTP-1-3003, White paper to Address Contamination Issues in TEF, E.F. Love, 2008.

11. SRNL-LM200-2009-00013, Recommendations for TEF to Minimize Further Contamination of $^{65}$Zn, Paul Korinko, Robert Malstrom, and Andrew Duncan, 4/2009.
12. SRNL-L7100-2010-00008, Examination of TEF Filters for $^{65}$Zn Trapping, Paul Korinko, Michael Tosten, Zane Nelson, 2/2010.
13. SRNL-L7100-2010-00034, Examination of New Filter Media used for Zn Coalescing Filters, Paul Korinko, 8/2010.
14. SRNL-L7100-2010-00019, $^{65}$Zn Trapping and Containment Optimization, P. Korinko, 5/2010.